Foraminifera on the deep-sea floor: lysocline and dissolution rate

Dissolution
Foraminifera
Deep-sea carbonates
Lysocline
Ontong-Java Plateau

Dissolution
Foraminifères
Carbonates océaniques
Lysocline
Plateau d'Ontong-Java

W. H. Berger [a], M.-C. Bonneau [b]*, F. L. Parker [a]
[a] Scripps Institution of Oceanography, La Jolla, California, USA.
[b] Département de Géologie dynamique, Université Paris VI, 4, place Jussieu, 75230 Paris.
* Present address: Compagnie Française des Pétroles, 39-43 Quai André-Citroën, 75739 Paris Cedex 15.

Received 15/9/81, in revised form 23/12/81, accepted 30/12/81.

ABSTRACT

The state of preservation of foraminiferal assemblages in a region of the western equatorial Pacific, combined with data on carbonate and ^{14}C sedimentation rates, suggest the following: 1) dissolution effects are noticeable but minor above 3 000 m depth; 2) the lysocline is near 3 400 m and straddles a marked increase in the rate of carbonate dissolution; 3) the loss of carbonate here is 15 to 20%; 4) only residual assemblages occur below 4 km depth, and these are not very sensitive to additional dissolution. A "linear" model of calcite dissolution with a defined zero loss near 3 km and 100% loss at the CCD provides a reasonably good approximation to the lysocline model which fits the data. The most sensitive preservation indices are fragmentation in the fine sand fraction, and changes in faunal composition of the fraction greater than 150 μm.

Oceanol. Acta, 1982, **5**, 2, 249-258.

RÉSUMÉ

Foraminifères sur les fonds océaniques: lysocline et taux de dissolution

Les variations de l'état de préservation des assemblages de foraminifères, des teneurs en carbonates, et des taux de sédimentation (^{14}C) dans la région ouest-équatoriale du Pacifique suggèrent que: 1) les effets de la dissolution sont visibles mais mineurs à des profondeurs inférieures à 3 000 m; 2) la lysocline se situe autour de 3 400 m et correspond à un accroissement marqué de la vitesse de dissolution des carbonates; 3) la perte de carbonate à ce niveau est de 15 à 20%; 4) aux profondeurs supérieures à 4 000 m, seuls les assemblages résiduels sont présents, et ceux-ci sont peu sensibles à une augmentation de dissolution.
Un modèle "linéaire" de dissolution de la calcite avec un zéro pris à environ 3 000 m et 100% de perte à la profondeur de la "CCD" représente une bonne approximation du modèle de "lysocline" basé sur les données. Les indices de préservation les plus sensibles sont la fragmentation dans les fractions fines et les variations de composition des assemblages planctoniques de la fraction supérieure à 150 μm.

Oceanol. Acta, 1982, **5**, 2, 249-258.

INTRODUCTION

The preservation of foraminifera on the deep-sea floor has attracted increased attention over the last ten years, mainly for three reasons:

1) The state of preservation in surface sediments reflects the physico-chemical conditions of sedimentation (including state of saturation and bottom current activity); 2) the state of preservation varies considerably through time, and provides a stratigraphic tool of high precision (the control of CO_2 content of the atmosphere over geologically short time spans is of special interest in this context); 3) an interpretation of fossil foraminiferal assemblages in terms of

paleotemperature or other parameters of shell production needs to take into account preservational state (this is true both for statistical analysis and for isotopic analysis).

The concept of the lysocline has proved useful in this context. As originally defined (Berger, 1968) it describes a depth level separating well preserved from poorly preserved assemblages. It is also thought to denote a level where dissolution rates increase strongly (Berger, 1970). Recently, this interpretation has been questioned (Clochiatti, 1980). Here we present information which helps resolve the problem of the relationship between lysocline and dissolution rate distribution. The various problems associated with foraminiferal preservation and recent progress in this field of research have been reviewed elsewhere (Volat *et al.*, 1980; Berger, 1981; Thunell, Honjo, 1981; Thunell *et al.*, 1981; Vincent, Berger, 1981). Here we focus on a detailed preservational depth profile in a deep-ocean region away from the continents and hence away from the disturbances introduced at their margins (Kennett, 1966; Berger, Soutar, 1970; Moore *et al.*, 1973; Thiede, 1973; Berger, 1978; Swift, Wenkam, 1978). In order to depict the present (i.e. late Holocene) situation, we have studied samples from the surface of large-volume box cores. All these cores are dated by ^{14}C analysis. The area where the box cores were taken, the Ontong-Java Plateau, has been studied both geophysically and sedimentologically (see Johnson *et al.*, 1977), and from the point of view of Pleistocene oxygen isotope cycles (Shackleton, Opdyke, 1973; 1976) and dissolution cycles (Thompson, 1976). Previously published preservational profiles, in general, are based on scattered undated samples plotted on rather large regions (review in Sliter *et al.*, 1975 and Belyaeva, 1980; exceptions are provided by Valencia, 1973; and Melguen, Thiede, 1974). The importance of dating surface sediments in order to avoid mapping fossil carbonates is evident from the study of Broecker and Broecker (1974).

The goal is to assess quantitatively the amount of dissolved carbonate in foraminiferal ooze, from the study of preservational state (Thunell, 1976; Ku, Oba, 1978). The present paper is a contribution toward this goal.

MATERIALS, METHODS, AND DATA TABULATION

The box cores studied (Eurydice Expedition of Scripps Institution of Oceanography, Leg 9, April, 1975) range in depth from 1 598 m to 4 441 m. They are all within a few degrees of one another (Tab. 1, Fig. 1). As retrieved, the box cores measure 50 × 50 cm in the horizontal plane, and they are optimally near 45 cm deep. The subcores, from which our samples were taken, consist of cylindrical sections extracted from the box core by pushing a sharp-edged plastic tube vertically downward into the box. A certain amount of foreshortening is observed during this operation (∼ 10%), but the surface sediment is well retained and the stratification is not disturbed. The subcores are 8 cm thick and near 40 cm long. The sediments here analyzed represent the uppermost 2 to 3 cm of such subcores.

Carbonate percentages are high, ranging from 71% to 88% (Tab. 2 and Fig. 2). Maximum sand content (foraminifera) reaches 64%. It decreases with increasing depth of water, and falls to 7% in the deepest samples. This phenomenon was observed previously and ascribed to the effects of winnowing on the top of the plateau and to the breakdown of shells at depth (Berger, Johnson, 1976; Johnson *et al.*, 1977; Berger, Mayer, 1978). The exact sand content measured in the partially dissolved samples depends not only on the preservation state but also on the intensity of the mechanical sieving operation. It is important, therefore, to standardize the sieving procedure. The grain-size data here presented (Tab. 2 and Fig. 3) fulfill this condition.

For grain-size analysis, the samples were treated as follows: one gram of dry sample was disaggregated in water and subjected to a few seconds (∼ 6) of ultrasonic treatment. It was then wet-sieved under a weak spray of water. Each size class (0.4 μm – 20 μm, 20-40, 40-63, 63-80, 80-100, 100-125, 125-150, 150-250, 250-315, 315-400 and > 400 μm) was dried and then weighed. Total losses due to procedure were between 1 and 2%. Replicates showed less than 2% difference in weight. Further details may be found in Bonneau (1978), and in Bonneau *et al.* (1980 *a*, *b*).

Table 1

Location of ERDC box cores and supplementary data ($CaCO_3$ from Johnson et al., 1977; *^{14}C data from Berger and Killingley,* 1982*). $CaCO_3$ values refer to the upper* 10 *cm (usually* 2 *to* 7 *cm). ^{14}C values refer to the mixed layer (usually* 0-5 *cm). ^{14}C-derived sedimentation rates are estimates derived from* 3 *dates and calculated using a mixing model. They agree well, in most cases, with the faunally derived estimates of Johnson* et al., 1977 *(except for Cores* 123 *and* 125*). Ages marked (?) or ( ) do not refer to a mixed layer (which is poorly developed in these cores) but are the probable age of uppermost sediment.*

Core No.	Depth (m)	Latitude	Longitude (E)	$CaCO_3$ %	Sand (%) > 63 μ	Sand (%) > 150 μ	Age (10^3yr)	Rate (cm/10^3yr)
ERDC 92 Bx	1 598	2°13.5'S	156°59.9'	82.8	64	47	4.4	1.6
ERDC 88 Bx	1 924	0°02.9'S	155°52.1'	88.1	55.5	41.5	4.8 (?)	1.2
ERDC 112 Bx	2 169	1°37.5'S	159°14.1'	85.5	58	42	4.3	2.0
ERDC 120 Bx	2 247	0°01.0'S	158°41.6'	83.9	45	37	3.9	2.05
ERDC 79 Bx	2 767	2°47.1'N	156°13.8'	85.4	39	30	4.4	1.7
ERDC 123 Bx	2 948	0°01.3'S	160°24.9'	83.5	35	28	3.4	2.1
ERDC 125 Bx	3 368	0°00.2'S	160°59.9'	82.8	29.5	23.5	3.4	2.2
ERDC 135 Bx	3 509	0°52.5'N	160°59.6'	82.5	24	17.5	4.5	1.4
ERDC 128 Bx	3 732	0°00.3'S	161°25.6'	81.6	19	13.5	4.0	1.7
ERDC 136 Bx	3 848	1°06.0'N	161°36.3'	79.6	8.5	5.2	4.3	1.4
ERDC 129 Bx	4 169	0°00.4'S	161°58.5'	78.7	9.5	5.5	4.3 (?)	0.8 (?)
ERDC 141 Bx	4 324	2°21.7'N	163°42.4'	82.4	7	2.5	(< 6)	∼ 0.6
ERDC 131 Bx	4 441	0°01.6'S	162°41.1'	71.3	7	3.25	6.3	0.85

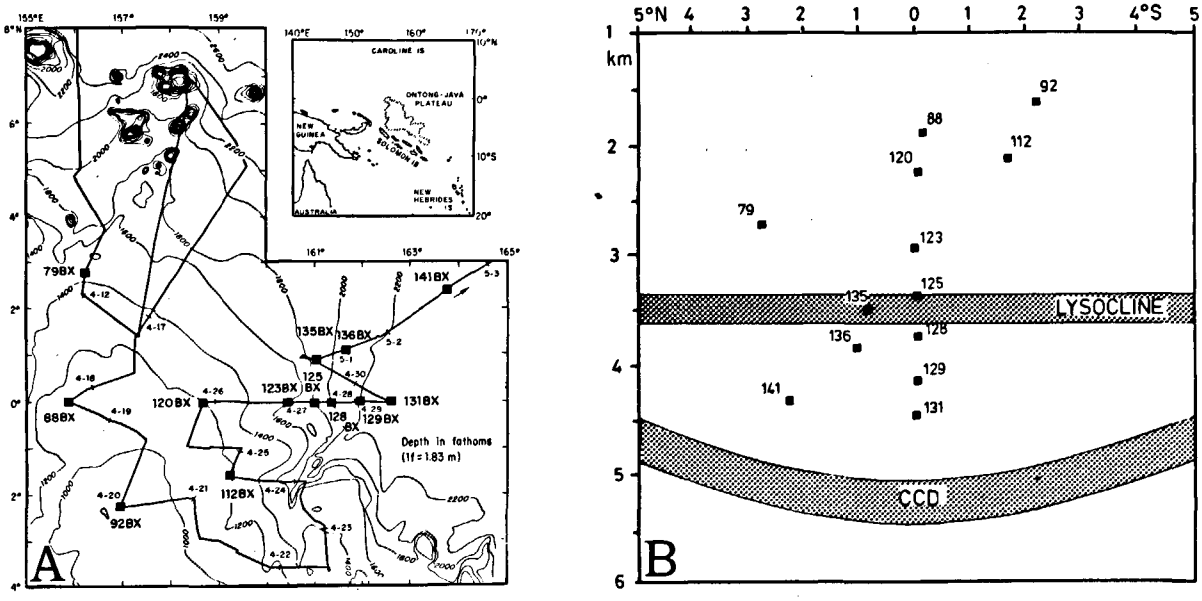

Figure 1

a. Location map, western equatorial Pacific (from Johnson et al., 1977). *b. Distribution of ERDC box cores in a latitude-depth frame. Lysocline and CCD position as defined prior to this study (Parker, Berger,* 1971; *Valencia,* 1973; *Berger,* 1977; *Berger, Killingley,* 1982*). The term "lysocline" refers to a marked change in faunal composition, the "CCD" is the carbonate-depth intersect.*

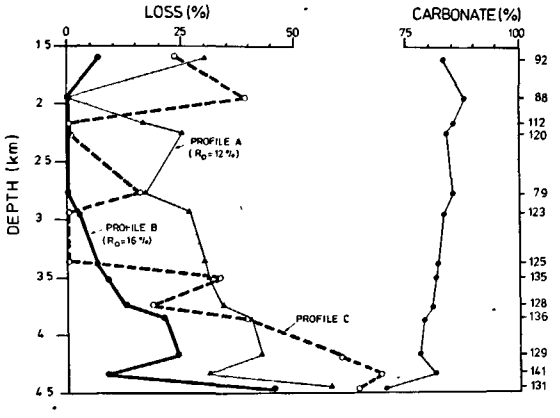

Figure 2

Carbonate content and interpretation in terms of loss to dissolution (left), assuming R_0 = 12% (Profile A) and R_0 = 16% (Profile B), where R_0 is the insoluble residue. Profile C shows the carbonate loss calculated by using ^{14}C sedimentation rates.

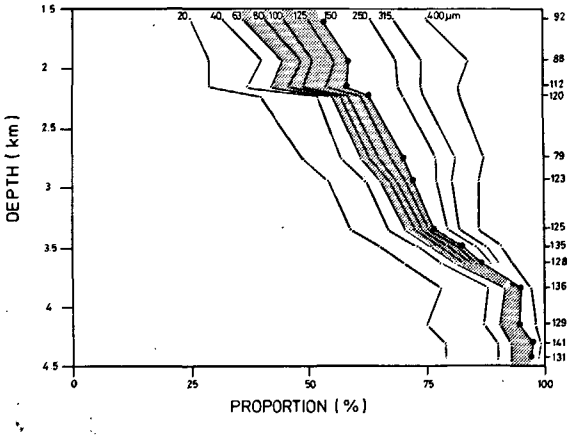

Figure 3

Abundance distribution of size classes as a function of water depth. Size classes were determined by sieving. Shaded area is the "small foraminifera" fraction of Parker and Berger (1971).

Table 2

Grain size analyses of ERDC box cores. Cores listed according to depth. Entries are in weight percent of sample in each grain size interval. These data are plotted in Figure 3.

Core	Depth (m)	<20 µm	20-40 µm	40-63 µm	63-80 µm	80-100 µm	100-125 µm	125-150 µm	150-250 µm	250-315 µm	315-400 µm	>400 µm
92 Bx	1 598	25	7	4	5	4	5	3	10	5	7	25
88 Bx	1 924	29	11	4.5	4	2.5	4.5	3	10	5.5	10	16
112 Bx	2 169	29	8	5.0	4	3	5	4	11	5	8	18
120 Bx	2 247	40	12	3	2	1.5	2.5	2	7	4.5	7.5	18
79 Bx	2 767	49	8	4	2	2	2.5	2.5	7	4	6	13
123 Bx	2 948	54	8	3	2	1.5	2	1.5	5	3.5	5.5	14
125 Bx	3 368	59	8	3.5	2	1.5	1.5	1	3	2.5	4	14
135 Bx	3 509	65	8	3	2	1.5	2	1	3	2	3	9.5
128 Bx	3 732	70	8	3	2	1.5	1	1	2	1.5	3	7
136 Bx	3 848	78	10	3.5	1.5	1	0.5	0.3	0.5	0.5	1.2	3
129 Bx	4 169	75	12	3.5	1.5	1	1	0.5	1.5	1	1	2
141 Bx	4 324	79	11	3	1.5	1.5	1	0.5	0.5	0.5	0.5	1
131 Bx	4 441	79	11	3	1.5	1	0.75	0.5	1	0.25	0.5	1.5

Foraminiferal counts were done both on the entire fraction > 150 µm (by F.L.P.) and on selected size classes within this fraction (by M.-C.B.). The taxonomy follows that of Parker (1962). When counting, only tests which represented at least two-thirds of a whole shell were considered. The counts for the fraction >

Table 3

Percentage of planktonic foraminifera in surface samples from ERDC box cores, in the fraction > 150 μm. Counts by F. L. Parker. Box cores are arranged in the order of water depth. Species are listed from least resistant (1) *to most resistant* (16)*, based on depth distribution in the present data. The order is somewhat different from that in Parker and Berger* (1971) *and in Berger* (1971). 1. *rbs* = G. rubescens; 2. *tnl* = G. tenellus; 3. *rbr* = G. ruber; 4. *glt* = G. glutinata; 5. *b+c* = G. bulloides, G. calida; 6. *sip* = G. siphonifera (= G. aequilateralis); 7. *sac* = G. sacculifer; 8. *cgm* = G. conglomerata; 9. *uni* = O. universa; 10. *cgb* = G. conglobatus; 11. *hum* = T. humilis; 12. *dtr* = N. dutertrei; 13. *clt* = G. cultrata (= G. menardii); 14. *obl* = P. obliquiloculata; 15. *tum* = G. tumida; 16. *deh* = S. dehiscens.

Core	Depth (m)	1 rbs	2 tnl	3 rbr	4 glt	5 b+c	6 sip	7 sac	8 cgm	9 uni	10 cgb	11 hum	12 dtr	13 clt	14 obl	15 tum	16 deh	Σ	Shells counted
92 Bx	1 598	7	4	34	26	7	6	7	1	.1	1	.1	3	.1	4	.3	.1	100.7	727
88 Bx	1 924	8	4	28	33	8	4	5	.4	—	.4	1	4	.4	4	—	.1	100.3	560
112 Bx	2 169	6	1	35	27	9	8	6	2	—	1	.3	1	.1	3	.3	—	99.7	355
120 Bx	2 247	4	1	27	14	7	10	15	2	.2	2	1	3	.5	12	1	.1	99.8	605
79 Bx	2 767	3	1	28	27	8	8	12	.2	—	1	2	3	1	7	.2	—	101.4	519
123 Bx	2 948	1	.2	18	25	14	11	12	2	.2	1	3	3	1	7	.2	.2	98.8	508
125 Bx	3 368	—	—	3	11	10	9	13	3	—	1	5	5	2	35	2	.5	99.5	367
135 Bx	3 509	—	—	2	.4	3	11	11	2	.2	.6	1	6	2	56	3	1	99.2	465
128 Bx	3 732	—	—	—	.2	1	8	6	.6	.2	1	—	8	2	67	4	2	100.0	663
136 Bx	3 848	—	—	—	.6	—	.6	2	.3	—	—	1	6	1	82	6	.6	100.1	311
129 Bx	4 169	—	—	.2	.2	.2	.6	1	.3	—	—	—	3	1	78	11	5	100.5	659
141 Bx	4 324	—	—	—	.3	1	4	2	—	—	2	.3	10	2	69	6	2	100.6	288
131 Bx	4 441	—	—	—	.4	—	.4	.4	.4	—	—	.4	5	3	75	12	3	100.0	245

Table 4

Percentages of dominant planktonic foraminifera, foram fragments, and opaline skeletons, in 3 size fractions of surface samples from ERDC box cores. Counts by M.-C.B. Cores arranged according to water depth. sip = G. siphonifera; *sac* = G. sacculifer; *obl* = P. obliquiloculata; *clt* = G. cultrata, *tum* = G. tumida; *oth = other; frg = fragments; op = opal;* Σ = *total particles counted.*

	Size class > 400 μm								*Size class 400-315 μm*								
Cores	sip	sac	obl	clt + tum	oth	frg	op	Σ	rbr	sip	sac	obl	clt + tum	oth	frg	op	Σ
92 Bx	4	18	51	3	16	8	—	293	6	16	25	17	2	17	17	—	337
88 Bx	4	14	57	7	9	9	—	680	6	18	29	19	3	10	15	—	734
112 Bx	7	15	56	6	11	5	—	390	6	18	28	21	1	16	10	—	370
120 Bx	5	11	57	5	13	9	—	450	5	16	23	18	3	16	19	—	304
79 Bx	2	12	55	10	14	7	—	321	5	12	29	19	3	10	22	—	370
123 Bx	4	7	59	7	9	14	—	627	1	10	16	18	2	13	40	.1	599
125 Bx	1	1	63	5	6	24	—	370	—	3	11	22	2	5	57	.3	393
135 Bx	2	1	58	5	7	27	—	336	—	2	5	19	2	4	68	—	394
128 Bx	.4	—	49	7	6	37	.2	617	—	1	.6	25	4	9	60	.6	534
136 Bx	—	—	49	6	5	40	—	334	—	—	.7	33	4	3	58	1	410
129 Bx	—	—	54	6	4	35	1	170	—	.2	—	15	2	2	80	1	423
141 Bx	—	—	61	2	3	31	3	116	—	—	—	27	5	6	52	10	110
131 Bx	—	—	62	3	3	32	.5	200	—	.3	—	52	3	2	42	1	297

Size class 315-250 μm								
rbr	*sip*	*sac*	*obl*	*clt+ tum*	*oth*	*frg*	*op*	Σ
26	12	22	4	1	16	19	—	340
25	17	20	6	1	10	21	.5	537
26	14	21	5	1	13	20	.5	400
20	14	22	5	1	12	26	.3	355
18	13	19	4	2	10	34	—	462
6	16	15	4	.5	10	48	—	406
—	6	9	3	.2	7	74	1	414
—	3	5	5	.3	5	81	.8	382
—	1	2	5	.6	1	86	4	477
—	3	2	11	—	7	71	6	219
—	—	.7	1	1	1	84	12	421
—	—	—	10	—	6	62	22	68
—	—	—	4	2	10	77	7	141

150 μm are given in Table 3. Counts by size class are listed in Table 4. These counts refer to the first five dominant species only and include counts on fragments and siliceous tests. Siliceous tests are included because, as a residual fraction concentrated by carbonate dissolution, their abundance contains information on the amount of such dissolution. The data are plotted in Figure 4, upper part. Counts not distinguishing species are shown in Figure 4, lower part. Detailed counts by size classes were done on 4 samples (88, 128, 123, 131) which represent distinct states of preservation. These are not listed but are summarized in Figure 5.

RESULTS

Carbonate percentages

The carbonate values (determined by measuring the pressure of CO_2-gas in a "bomb", see Johnson *et al.*, 1977) range from 71.3% to 88.1%. We can determine the apparent loss of carbonate from dissolution using the equation (Berger, 1971)

$$L = 1 - R_0/R, \qquad (1)$$

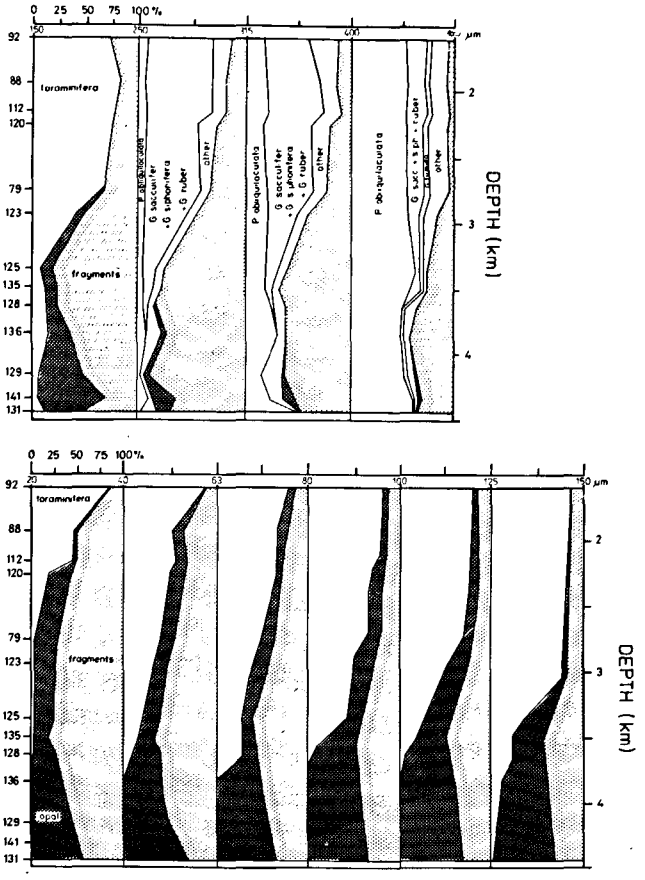

Figure 4
Distribution of fragments in various size fractions as a function of water depth.

based on its ^{14}C stratigraphy (see Berger, Killingley, 1982). ERDC 120 Bx is the shallowest one of the equatorial cores with a high sedimentation rate. Its carbonate content of 83.9% is close to the average of supra-lysoclinal cores, down to the depth of 3 368 m (ERDC 125 Bx). Therefore, we prefer to take the percentage of the non-carbonate in Core 120 as R_0 (= 16%). The resulting loss profile (Fig. 2, Profile B) agrees much better than Profile A with the other data available.

The Loss Profile B suggests that serious dissolution of carbonate only occurs below 3 000 m depth, and that dissolution rates then increase exponentially with depth, doubling every 500 m or so. The anomalous point at 4 324 m (9% loss) belongs to ERDC 141 Bx, which has no mixed layer, and whose upper 5 cm of sediment have an average age of about 7 300 ^{14}C years.

We can check whether the Loss Profile B is plausible, using the ^{14}C-sedimentation rates (Tab. 1). The carbonate sedimentation rates can be interpreted in terms of carbonate loss by calculating

$$L = (S_0 - CaCO_3\% \times S)/S_0 = 1 - CaCO_3\% \times S/S_0, \quad (2)$$

where S_0 is the standard rate of undissolved carbonate, and S is the individual sedimentation rate of a core. Setting S_0 = 1.72 (based on Core 120, as before) we obtain yet another loss profile (Fig. 2, Profile C).

The general pattern of Profile C is in agreement with Profile B: both suggest that there is very little loss of

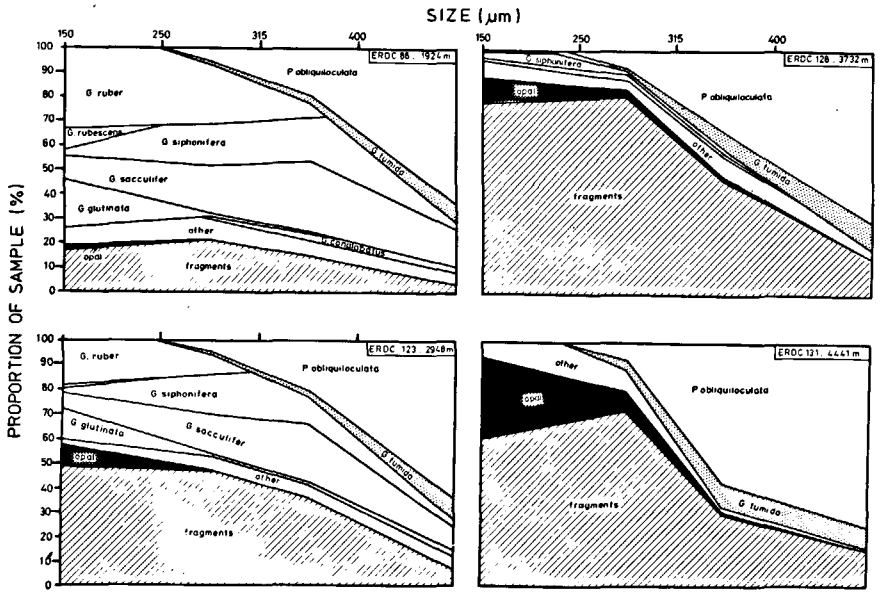

Figure 5
Progressive changes in fossil assemblages within various size fractions due to carbonate dissolution, illustrated with 4 samples from various depths. Counts by M.-C. B.

where R_0 is the initial insoluble residue, in percent, and R is the residue after dissolution took place. Such a calculation was also made by Johnson *et al.* (1977).These authors assumed R_0 = 12%, taking the minimum residue value, that is, that of ERDC 88 Bx. The resulting loss profile shows considerable apparent dissolution at all depths except near 2 000 m (Fig. 2, Profile A). This profile is probably unrealistic. Armed with the ^{14}C-based sedimentation rates we can argue that the cores with the highest rates should provide the standard, not the one with highest $CaCO_3$ content. Also, we can exclude ERDC 88 Bx, as being disturbed, carbonate (or none) down to between 3 and 3.5 km depth. Below this depth losses increase rapidly. The loss values for the shallowest core (ERDC 92 Bx) are readily explained by winnowing processes evident from the high sand content here. The values for Core 88 are not comparable, as the core is disturbed (it probably suffered erosion; see Berger, Killingley, 1982). The "loss" value of 16% for ERDC 79 Bx refers to a core which was taken well away from the equator, and presumably shows relatively low sedimentation rates due to decreased productivity. Thus, the anomalies do not invalidate the impression that appreciable car-

bonate loss from dissolution begins below 3 km depth. This result, of course, refers to *calcite,* as there is no aragonite visible in any of the cores except the shallowest one.

One other observation is of interest. The losses in the deepest cores as calculated from differences in sedimentation rates exceed those calculated from the change in carbonate values. A general downslope "drift" of coccolith carbonate, from bioturbation and resuspension, could conceivably cause the effect. Clearly, if we wish to isolate the effects of dissolution from the various other phenomena (winnowing, erosion, bioturbation and sediment "drift") we need to turn to more sensitive properties than $CaCO_3$-content.

Grain size

The proportions of the various size classes change with depth of sediment sample (Fig. 3). The shallowest samples have a high proportion of coarse sediment, the deep ones are highly enriched in fine material. The sedimentation rates (Tab. 1) indicate that the fraction > 150 μm, for example, accumulates at a rate near 0.6 cm/10^3 yrs in the depth interval 2 to 3 km (product of rate and percent fraction). Below 4 km, it accumulates at a rate near 0.04 cm/10^3 yrs: less than 10% of the original rate. Despite its gain in proportion, the fine fraction also shows considerable net loss. Between 2 and 3 km, the fine fraction rate is near 1.4 cm/10^3 yrs. Below 4 km, the rates are between 0.6 and 0.7 cm/10^3 yrs: less than one-half of the original one.

Can we conclude from this that the fine fraction dissolves 5 times more slowly than the coarse fraction? Not so. Small foraminifera apparently are *more* susceptible to dissolution than large ones (see also Parker and Berger, 1971). Thus, there is a considerable transfer of shell fragments from the coarser fractions to the finer ones, as dissolution proceeds. This means that only the coarsest fractions feel the full impact of loss from dissolution, while the finer ones have both gains and losses. It also means that the total loss of carbonate will be considerably less than that calculated from coarse fraction losses alone, that is, from foraminiferal data. Conversely, the overall loss will be underestimated when based on the fine fraction alone. The oft repeated (and rarely supported) assertion that coccoliths are more resistant to dissolution than foraminifera may derive at least in part from the observation that the fine fraction is proportionally enriched in partially dissolved samples, and that the fine fraction is rich in coccoliths. As dissolution proceeds, of course, the proportion of coccoliths to unidentifiable fragments will decrease, but this may not be immediately apparent.

Transfer from coarse to fine fraction

From the change in sedimentation rates (Tab. 1) we can make a rough estimate of fragmentation transfer. Sedimentation rates decrease by a factor of 3, in going from shallow to deep cores (2-2.5 km vs. 4-4.5 km). Carbonate percentages (Tab. 1) change from, say, 84% to 77%. We conclude that 70% of the carbonate initially sedimented has been lost (see schedule).

Assume that this 70% loss from dissolution occurs in all fractions equally. Then, without size transfer, we should expect no change in proportions. In fact, the sand fraction decreased from 50 to 8 percent (Tab. 1) and the finest fraction (< 20 μm) increased from 35 to 78 percent (Tab. 2). Of the initial 50 parts per hundred in the coarse fraction, 35 (= 70%) were dissolved by our assumption. Only 2.4 (= 8 × 1/3) are left, hence 12.6 parts were passed on as fragments. Of the initial 22 parts per hundred carbonate in the finest fraction, 15.4 (= 70%) were dissolved, but we find 20.3 (= 61 × 1/3) instead of the expected 6.6. Hence, about 14 parts were gained. The mid-fraction (20-63 μ) shows but little change in proportion: apparently losses and gains of particles were almost balanced, although a certain loss of carbonate is evident because of the increase in opal proportion. Overall, about 1/7 of the initial sediment passed from sand fraction to the finest fraction, as fragments, during the dissolution of 70% of the carbonate initially deposited.

That fragments move from coarser to finer size classes as dissolution progresses, is obvious under the microscope. To this evidence we turn next.

Schedule for fragment transfer calculation (see Tab. 1 for data)

	Shallow (2-2.5 km)	Deep (4-4.5 km)	Units
Sedimentation rate	2	2/3	cm/1 000 yrs
Carbonate	84	77	% of total sediment
Carbonate rate	1.7	0.5	cm/1 000 yrs
Factor	1	0.3	
Loss	0	0.7	
Sand fraction (> 63 μm)	50	8	% of total sediment
Finest fraction (< 20 μm)	35	78	% of total sediment
Sand fraction carbonate*	50	8	% of total sediment
Finest fraction carbonate*	22	61	% of total sediment

* assumed, based on the observation that most of the non-carbonate matter present is in finest fraction (with values estimated as 13% of 16% for shallow, and 17% of 23% for deep).

Fragmentation

The distribution of fragments, as a function of depth, shows a characteristic pattern with depth (Fig. 4). Three types of particles make up the classes greater than 20 μm; whole foraminifera, fragments of foram tests, and siliceous tests (diatoms, radiolarians). The fine silt and clay fractions (< 20 μm) consist mainly of coccolithophores and foram fragments, as well as siliceous tests and clay minerals. Only the fractions greater than 20 μm are treated here. The classes greater than 150 μm are referred to as « coarse », those with particles smaller than this as « fine ».

The trends of fragmentation in the coarse fractions (Fig. 4, upper graph) are quite clear. Whole foraminifera dominate above 3 km depth, fragments dominate below 3.3 km depth. Distinct changes in faunal composition accompany the progressive fragmentation. Within the coarse fraction, the coarser ones show the lesser effect. This trend is as expected, if the coarser fractions deliver fragments to the finer ones and if the ease with which fragments are produced slows as the more fragile species are removed.

From inspection of the fragment distributions in the coarse fractions we may draw the following conclusions :

1) a low proportion of fragments is always present, even when no appreciable dissolution has occurred;

2) the proportion of coarse fraction fragments is a sensitive dissolution index, at and somewhat above the lysocline: it is not a good index below the lysocline;

3) within the sand sizes, the finer the size, the more sensitive it is to changes in preservation state.

Similar conclusions apply to the size classes smaller than 150 μm (Fig. 4, lower graph). In the medium-sized foraminifera (125-150 μm) the fragmentation index shows an excellent correlation with depth (r = .94). The index is calculated as

$$F\,(\%) = 100 \times \text{fragments}/(\text{fragments} + \text{whole tests}). \quad (3)$$

The regression equation [depth = (F + 39)/0.0273] yields the correct depth within 250 m, on the average. The excellent correlation between F (125-150 μm) and water depth establishes this index as an important tool for dissolution studies.

Inspection of the distribution of particles in the fine fractions (Fig. 4, lower graph) suggests the following: 1) whole tests disappear rapidly below 3 500 m, so that most fragments must be delivered from the coarser fractions in the deep samples, as also seen in the microscope; 2) below 4 000 m the steady state between delivery and dissolution of fragments is reached at progressively lower carbonate values, suggesting increased resistance of residual fragments to dissolution; 3) the amount of non-carbonate becomes a good index of dissolution under these conditions, in these size fractions.

Foraminiferal assemblages

Each size fraction has a different composition of foraminiferal species, and each size fraction therefore reacts differently to the attack by carbonate dissolution.

The general trends of faunal change are exemplified in Figure 5, which shows a selection of 4 assemblages from various depths. The shallowest of these assemblages (ERDC 88, 1 924 m) is typical for the composition of the undissolved foraminiferal fauna in this region. In the fraction 150-250 μm, *G. ruber* is dominant, in 250-315 μm that species is joined by *G. sacculifer* which becomes dominant in the fraction 315-400 μm. In the class > 400 μm *P. obliquiloculata* dominates. Besides these three species, *G. siphonifera, G. glutinata,* and *G. conglobatus* are abundant. The highly solution-sensitive species *G. rubescens* is common in the fraction 150-250 μm. There is an appreciable amount of fragments in all size fractions. The origin of these fragments is not clear; some may have been produced in the water column by predation, others by biological activity on the seafloor, and a portion may stem from the process of washing the samples.

The next deeper sample (ERDC 123, 2 948 m) shows much the same assemblage, except for a distinct increase in the proportion of fragments, indicating weakening of shells from dissolution effects. The fragments are largely from *Globigerinoides* species, which are quite susceptible to dissolution. Apparently the actual loss of carbonate which produces this weakening of shells is small: the sedimentation rate patterns (Tab. 1) do not reflect it.

The next deeper sample (ERDC 128, 3 732 m) clearly reflects the sublysoclinal position of the assemblage. The resistant forms *P. obliquiloculata* and *G. tumida* dominate the residual assemblage, and fragments are extremely abundant especially in the fraction 150-250 μm. These fragments are largely derived from the dominant species, the fragments of the more susceptible species having been dissolved or passed on to the finer size fractions. The deepest sample (ERDC 131, 4 441 m) shows much the same composition, with the additional change of greatly increased opal content. Here, then, the production of fragments is eclipsed by the strong dissolution of both shells and fragments, so that the carbonate content is appreciably decreased. All fragments in this deepest sample are derived from the large resistant foraminifera: *P. obliquiloculata, G. tumida* and *G. cultrata.*

The changes of foraminiferal assemblages in response to progressive differential dissolution can be expressed by various preservation indices. The simplest one of these indices is the percentage of resistant species (Ruddiman, Heezen, 1967):

$$R\,(\%) = \Sigma P_i;\ i = 1, m \quad (4)$$

where i is the code number of the species and 1 to m includes the solution-resistant forms. A sample might have the index "30", indicating that it has 30% resistant species (higher than normal for undissolved samples).

A somewhat more sensitive index is of the form of an average weighted mean of resistance ranks of the species (Berger, 1968; 1975 *b;* Adelseck, 1977) :

$$FDX = \Sigma r_i P_i / \Sigma P_i; \; i = 1,n. \qquad (5)$$

Here r_i is the rank, with respect to dissolution susceptibility, of the species i and P_i denotes the proportion in the assemblage. If all species are used, P_i equals unity. Instead of "species", we can also read "group of species", if several species are assigned the same rank. A sample might have the index "11", indicating that the overall average rank with respect to dissolution is 11. If "1" stands for most susceptible, and "15" for most resistant, the index "11" suggests enrichment in resistant species at the expense of susceptible ones.

Another way of indexing a sample for preservation state is to calculate a similarity to an undissolved assemblage (Berger, Soutar, 1970).

The simplest similarity equation is of the form :

$$S = \Sigma \min (P_{ij}, P_{ik}); \; i = 1,n \qquad (6)$$

where i stands for species, as before, j stands for the sample being indexed and k stands for the reference sample.

We have calculated preservation indices according to equations 4 and 5. The depth profiles are shown in Figure 6. The dissolution ranking of species is that shown in Table 3. The profiles of the dissolution indices (Fig. 6, upper graph) show that the samples above 3 km depth have well-preserved assemblages, whereas those below 3.7 km are greatly affected by dissolution. The changeover from "well preserved" to "poorly preserved" depends on the size fraction considered and

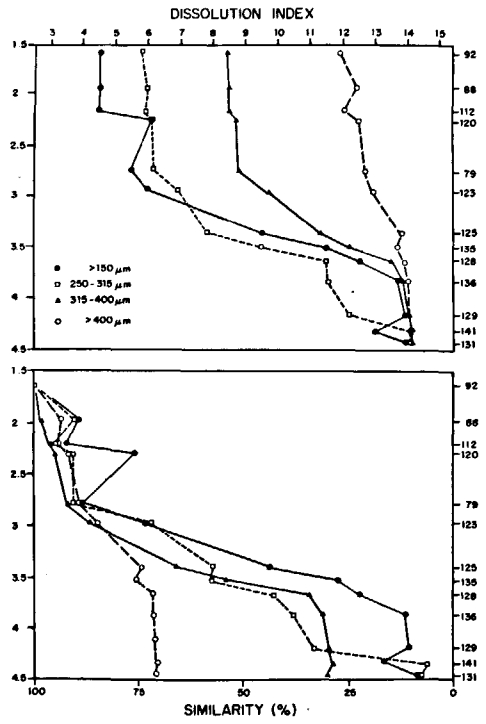

Figure 6

Depth profiles of dissolution indices for foraminifera assemblages of each size fraction. Fraction > 150 µm: counts by F.L.P. (see Tab. 3). All others: counts by M.-C.B. (dominant species only, Tab. 4). Upper: index represents the weighted average rank with respect to resistance $\Sigma r_i P_i$; lower index represents similarity to a standard undissolved assemblage (see text).

lies somewhere between 3 300 and 3 500 m. The most sensitive fraction (the one with the largest range of indices and with some gradient seen in the "well preserved" and the "poorly preserved" set) is the sum fraction > 150 µm. This is due to the high species diversity in this group, and the fact that all species were counted. The indices of the other fractions are based on a short species list. Among these, the size class > 400 is the least sensitive one.

The similarity plot (with ERDC 92 Bx serving as standard, because of being shallow) shows that assemblages change very little down to ERDC 79 Bx at 2 767 m. The sample near 3 000 m (ERDC 123 Bx) shows the first distinct difference to the "standard", which is greater than might be expected from counting statistics and the difference in location. The next sample, at 3 368 m (ERDC 125 Bx) is distinctly different from the standard. Its similarity to the standard differs from the "shallow" set of samples (< 3 000 m) by about the same amount as it differs from the "deep" set (> 3 500 m). Hence, the halfway point between "well-preserved" and "poorly preserved" samples is near 3 400 m according to this similarity criterion, the same as for the dissolution index. The core ERDC 125 Bx, then, straddles the lysocline as originally defined (Berger, 1968), namely the boundary zone between good and poor preservation of foraminiferal assemblages.

Discussion

The meaning of the paleontologically defined concept "lysocline", or more specifically "foraminifera lysocline", in physico-chemical terms has been a matter of speculation and discussion (reviewed in Berger, 1975 *b*; see also Edmond, 1974; Clochiatti, 1976; Leclaire, Clochiatti, 1976; Adelseck, 1977; Broecker, Takahashi, 1978; Ku, Oba, 1978). We can now state unequivocally that in our data there is no evidence for appreciable calcite dissolution above the lysocline : the crucial lysocline sample from ERDC 125 Bx with its high carbonate value and its high sedimentation rate belongs to the "shallow" group of cores from a purely physical viewpoint (Tab. 1; Fig. 2, Profile C).

It is clear, however, that *some* calcite dissolution must occur above the lysocline, in order to produce the trends in fragmentation and in change of assemblage character which we have documented. The first distinctly noticeable change, on following the depth profiles of fragmentation and faunal composition, appears in Core ERDC 79 Bx, at 2 767 m. We suggest, therefore, that this core is somewhat below the R_0-level, the level down to which there is no change in species composition from dissolution (Berger, 1978). In the Atlantic this level is between 3.5 and 4 km in the open ocean; it apparently follows a depth of equal saturation (namely the one calculated to be zero by Takahashi, 1975; see Berger, 1977). In the Atlantic the lysocline is between 500 m and 1 000 m deeper than the R_0-level. If we take the R_0-level as 2 700 m in the present case, and the lysocline at 3 400 m, we obtain a difference of 700 m, which is within this same range.

Various dissolution profiles have been envisaged for various regions of the seafloor (Berger, 1970; 1981; Heath, Culberson, 1970; Clochiatti, 1980). Based on the data presented here (Fig. 2 to 6) we can now attempt to construct such a profile for the Ontong-Java Plateau. We proceed from the following observations and inferences: 1) there is some calcite dissolution seen even in the shallowest core, which lies well below the aragonite compensation depth. Dissolution takes place in organic-rich microenvironments and helps weaken some shells sufficiently so that they will disintegrate when stressed mechanically, for example by deposit-feeders (or during washing in the laboratory). However, above 2 500 m the actual loss of calcite-carbonate from dissolution is negligible, at most a few percent; 2) below 2 500 m the surrounding bottom water is close enough to undersaturation so that dissolution can proceed more readily within CO_2-rich microenvironments. The rate of fragment production increases slightly, and noticeable changes in species composition begin near 2 700 m. The loss of carbonate is still minor, down to 3 000 m; 3) below 3 000 m the disintegration of the foraminiferal assemblages begins in earnest. The midpoint between the original composition and one entirely dominated by a few resistant species is reached near 3 400 m. Down to this depth there is still relatively little apparent loss of carbonate. It is possible that whatever carbonate is lost to dissolution is resupplied from upslope areas by redeposition. Evidence for a more or less constant influx of redeposited carbonate in mid-depth sites has been presented elsewhere (Berger, Killingley, 1982; see also Moore *et al.*, 1973); 4) below the lysocline (at 3 400 m), the rate of dissolution of carbonate is high enough to overcome any effects of redeposition, and the sedimentation rates drop markedly. The faunal assemblages deteriorate rapidly below this depth; 5) below 4 000 m dissolution effects dominate, the faunas are residual and cannot change much in response to variations in dissolution intensity.

These various observations and propositions are summarized in Figure 7. Our profile of carbonate dissolution and its relationship to R_0-level, lysocline, and CCD, is in good general agreement with the lysocline models of Berger (1970) and of Berger *et al.* (1976) which are based on the experiments of Peterson (1966) and Berger (1967), and on scatter plots of dissolution indices versus depth, for large regions. It also, we believe, resolves the questions recently raised by Clochiatti (1976; 1980) regarding the nature of the lysocline. In agreement with her suggestion, for the purpose of carbonate budget calculations, our profile can be approximated by a model which postulates no

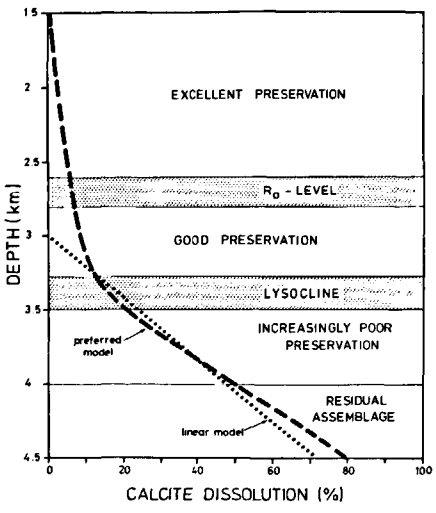

Figure 7

Model of relationship between foraminiferal preservation states and amount of calcite dissolution as a function of depth, proposed on the basis of carbonate contents, ^{14}C sedimentation rates, and foraminiferal compositions of ERDC surfaces samples. An "elbow" model with a defined zero loss at 3 km and within 100% loss at CCD (≈ 5 100 m) is a good approximation of our lysocline model.

dissolution above 3 km, and a linear increase in the rate of carbonate dissolution below that depth. Such an "elbow" model was earlier suggested by van Andel *et al.* (1975) who calculated the change in the depth gradient as a function of geologic time. Elbow models were also considered by Heath and Culberson (1970) and by Berger (1975 *a*; 1977). If we accept this model, the lysocline appears at a level where about 20% of the total carbonate has been lost to dissolution.

Our profile — slightly modified and quantified as compared with earlier open-ocean lysocline models (Berger, 1970; Berger *et al.*, 1976) — suggests total dissolution of carbonate at a depth near 4.8 km. This is 400 m shallower than the CCD for the region. We suggest that much of the carbonate below 4.8 km may be redeposited material or reworked older sediment which is being mixed with newly arriving carbonate but without a new sediment buildup. Only additional sampling can resolve this question.

Acknowledgements

W.H. Berger and F.L. Parker acknowledge support by the National Science Foundation (Oceanography Section Grants OCE 78-25587 and OCE80-24610) and by the Office of Naval Research (Contract N00014-80-C-0440). M.-C. Bonneau thanks Dr. Yves Lancelot for encouragement and advice during her work on this project.

REFERENCES

Adelseck C.G., 1977. Dissolution of deep-sea carbonate: preliminary calibration of preservational and morphologic aspects, *Deep-Sea Res.*, **24**, 1167-1185.

Belyaeva N.V., 1980. Polozhenie foraminiferovogo lizoklina v raznikh zonakh Tikhogo Okeana, *Litol. Polezn. Iskop., 1980 g*, **2**, 11-16 (Akad. Nauk SSSR).

Berger W.H., 1967. Foraminiferal ooze : solution at depth, *Science*, **156**, 383-385.

Berger W.H., 1968. Planktonic foraminifera: selective solution and paleoclimatic interpretation, *Deep-Sea Res.*, **15**, 31-43.

Berger W.H., 1970. Planktonic foraminifera: selective solution and the lysocline, *Mar. Geol.*, **8**, 111-138.

Berger W.H., 1971. Sedimentation of planktonic foraminifera, *Mar. Geol.*, **11**, 325-358.

Berger W.H., 1975 *a*. Dissolution of deep-sea carbonates: an introduction, *Cushman Found. Foraminiferal Res. Spec. Publ.*, **13**, 7-10.

Berger W.H., 1975 *b*. Deep-sea carbonates: dissolution profiles from foraminiferal preservation, *Cushman Found. Foraminiferal Res. Spec. Publ.*, **13**, 82-86.

Berger W.H., 1977. Carbon dioxide excursions and the deep-sea record: aspects of the problem, in: *The fate of fossil fuel CO_2 in the oceans*, edited by N. R. Andersen and A. Malahoff, Plenum Press, New York, 505-542.

Berger W.H., 1978. Sedimentation of deep-sea carbonate: maps and models of variations and fluctuations, *J. Foraminiferal Res.*, **8**, 286-302.

Berger W.H., 1981. Paleoceanography: the deep-sea record, in: *The Sea*, edited by C. Emiliani, Wiley-Interscience, New York, 1437-1519.

Berger W.H., Soutar A., 1970. Preservation of plankton shells in an anaerobic basin off California, *Geol. Soc. Am. Bull.*, **81**, 275-282.

Berger W.H., Johnson T.C., 1976. Deep-sea carbonates: dissolution and mass wasting on Ontong-Java Plateau, *Science*, **192**, 785-787.

Berger W.H., Mayer L.A., 1978. Deep-sea carbonates: acoustic reflectors and lysocline fluctuations, *Geology*, **6**, 11-15.

Berger W.H., Killingley J.S., 1982. Benthic mixing and ^{14}C sedimentation rates in the equatorial Pacific, *Mar. Geol.*, **45**, 93-125.

Berger W.H., Adelseck C.G. Jr., Mayer L.A., 1976. Distribution of carbonate in surface sediments of the Pacific Ocean, *J. Geophys. Res.*, **81**, 2617-2627.

Bonneau M.-C., 1978. Dissolution expérimentale et naturelle de foraminifères planctoniques : approches morphologiques, *Thèse 3e cycle, Univ. Pierre et Marie Curie, Paris*, 231 p.

Bonneau M.-C., Vergnaud-Grazzini C., Berger W.H., 1980 *a*. Stable isotope fractionation and differential dissolution in Recent planktonic foraminifera from Pacific box-cores, *Oceanol. Acta*, **3**, 3, 377-382.

Bonneau M.-C., Mélières F., Vergnaud-Grazzini C., 1980 *b*. Variations isotopiques (oxygène et carbone) et cristallographiques chez des espèces actuelles de foraminifères planctoniques en fonction de la profondeur de dépôt, *Bull. Soc. Géol. Fr.*, **22**, 791-793.

Broecker W.S., Broecker S., 1974. Carbonate dissolution on the western flank of the East Pacific Rise, in: *Studies in paleooceanography*, edited by W. W. Hay, Soc. Econ. Paleontol. Miner. Spec. Pub. No 20, 44-57.

Broecker W.S., Takahashi T., 1978. The relationship between lysocline depth and *in situ* carbonate concentration, *Deep-Sea Res.*, **15**, 65-95.

Clocchiatti M., 1976. Sédimentation pélagique Néogène et Quaternaire et dissolution des carbonates dans le bassin de Madagascar, *Bull. Soc. Géol. Fr.*, **18**, 1613-1624.

Clocchiatti M.D., 1980. Sédimentation carbonatée et paléoenvironnement dans l'Océan Indien au Cénozoique, *Thèse Doct. État, Mus. Natl. Hist. Nat. et Univ. Pierre et Marie Curie, Paris*, 143 p.

Edmond J.M., 1974. On the dissolution of carbonate and silicate in the deep ocean, *Deep-Sea Res.*, **21**, 455-480.

Heath G.R., Culberson C., 1970. Calcite: degree of saturation, rate of dissolution, and the compensation depth in the deep oceans, *Geol. Soc. Am. Bull.*, **81**, 3157-3160.

Johnson T.C., Hamilton E.L., Berger W.H., 1977. Physical properties of calcareous ooze: control by dissolution at depth, *Mar. Geol.*, **24**, 259-277.

Kennett J.P., 1966. Foraminiferal evidence of a shallow calcium carbonate solution boundary. Ross Sea, Antarctica, *Science*, **153**, 191-193.

Ku T.-L., Oba T., 1978. A method for quantitative evaluation of carbonate dissolution in deep-sea sediments and its application to paleoceanographic reconstruction, *Quat. Res.*, **10**, 112-129.

Leclaire L., Clocchiatti M., 1976. La dissolution des carbonates en milieu océanique. Son rôle dans la genèse des dépôts pélagiques pendant le Cénozoïque, *Bull. Soc. Géol. Fr.*, **18**, 1315-1335.

Melguen M., Thiede J., 1974. Facies distribution and dissolution depths of surface sediment components from the Vema Channel and the Rio Grande Rise (southwest Atlantic Ocean), *Mar. Geol.*, **17**, 341-353.

Moore T.C., Heath G.R., Kowsmann O., 1973. Biogenic sediments of the Panama Basin, *J. Geol.*, **81**, 458-472.

Parker F.L., 1962. Planktonic foraminiferal species in Pacific sediments, *Micropaleontology*, **8**, 219-254.

Parker F.L., Berger W.H., 1971. Faunal and solution patterns of planktonic foraminifera in surface sediments of the South Pacific, *Deep-Sea Res.*, **18**, 73-107.

Peterson M.N.A., 1966. Calcite : rates of dissolution in a vertical profile in the Central Pacific, *Science*, **154**, 1542-1544.

Ruddiman W.F., Heezen B.C., 1967. Differential solution of planktonic Foraminifera, *Deep-Sea Res.*, **14**, 801-808.

Shackleton N.J., Opdyke N.D., 1973. Oxygen isotope and paleomagnetic stratigraphy of equatorial Pacific core V28-238: oxygen isotope temperatures and ice volumes on a 10^5 year and 10^6 year scale, *Quat. Res.*, **3**, 39-55.

Shackleton N.J., Opdyke N.D., 1976. Oxygen-isotope and paleomagnetic stratigraphy of Pacific core V28-239 late Pliocene to latest Pleistocene, in: *Investigation of Late Quaternary Paleoceanography and Paleoclimatology*, edited by R.M. Cline and J.D. Hays, *GSA Mem.*, **145**, 449-464.

Sliter W.V., Bé A.W.H., Berger W.H., 1975. Dissolution of deep-sea carbonates, *Cushman Found. Foraminiferal Res. Spec. Publ.*, **13**, 1-159.

Swift S.A., Wenkam C., 1978. Holocene accumulation rates of calcite in the Panama Basin: lateral and vertical variations in calcite dissolution, *Mar. Geol.*, **27**, 67-77.

Takahashi T., 1975. Carbonate chemistry of sea water and the calcite compensation depth in the oceans, *Cushman Found. Foraminiferal Res. Spec. Publ.*, **13**, 11-26.

Thiede J., 1973. Planktonic foraminifera in hemipelagic sediments : shell preservation off Portugal and Morocco, *Geol. Soc. Am. Bull.*, **84**, 2749-2754.

Thompson P.R., 1976. Planktonic foraminiferal dissolution and the progress towards a Pleistocene equatorial Pacific transfer function, *J. Foraminiferal Res.*, **6**, 208-227.

Thunell R.C., 1976. Optimum indices of calcium carbonate dissolution in deep-sea sediments, *Geology*, **4**, 525-528.

Thunell R.C., Honjo S., 1981. Calcite dissolution and the modification of planktonic foraminiferal assemblages, *Mar. Micropaleontol.*, **6**, 169-182.

Thunell R.C., Keir R.S., Honjo S., 1981. Calcite dissolution: an *in situ* study in the Pacific Basin, *Science*, **212**, 659-661.

Valencia M.J., 1973. Calcium carbonate and gross-size analysis of surface sediments, western equatorial Pacific, *Pac. Sci.*, **27**, 290-303.

van Andel Tj.H., Heath G.R., Moore T.C., 1975. Cenozoic tectonics, sedimentation and paleo-oceanography of the central equatorial Pacific, *Geol. Soc. Am. Mem.*, **134**, 1-134.

Vincent E., Berger W.H., 1981. Planktonic foraminifera and their use in paleoceanography, in: *The Sea*, **vol. 7**, edited by C. Emiliani, Wiley-Interscience, New York, 1025-1119.

Volat J.L., Pastouret L., Vergnaud-Grazzini C., 1980. Dissolution and carbonate fluctuations in Pleistocene deep-sea cores: a review, *Mar. Geol.*, **34**, 1-28.